

OPERATION OF CUSPTRON OSCILLATOR FOR SIXTH HARMONIC FREQUENCY GENERATION WITH SIX-VANE CIRCUIT†

W. Namkung, J. Y. Choe, H. S. Uhm, and V. Ayres
Naval Surface Weapons Center, Silver Spring, Maryland 20903-5000

Abstract

Microwave radiation at high harmonics of the electron cyclotron frequency is generated from a cusptron device. An axis-rotating beam of 25-30 kV, 1.5-3.5 A, 4 μ s, and 60 pps interacts with modes in a six-vane circuit by the negative mass instability. Radiation power is more than 10 kW with approximately 10% electronic efficiency at 6.0 GHz which corresponds to the sixth harmonic of the electron cyclotron frequency. With the same circuit, we also obtained approximately 4.0 kW radiation with 9.5% efficiency at the fourth harmonic frequency of 3.9 GHz.

Introduction

A compact and high-power microwave and millimeter wave source is in great demand for various practical applications in particle accelerators, communications, radars, plasma heating, and others. Since most of high-power devices use electron beams and magnetic fields, operation at lower voltages and lower magnetic fields is required to be a compact device. Recently, there has been intense research on new high-power electro-magnetic radiation sources, e. g., gyrotrons, free electron lasers, and relativistic magnetrons. However, they use either high voltage beams requiring a bulky power supply and/or high magnetic fields commonly obtainable from superconducting magnets. Therefore, a device which operates at a high harmonic of the electron cyclotron frequency using a low energy beam holds promise as a compact and high-power tube.

Powerful microwave radiation has been observed from axis-rotating electron beams (E layers) in the Astron [1] for plasma confinements and in Electron Ring Accelerators [2] for collective ion accelerations. The interacting mechanism between E layers and the modes of the conducting boundaries has been identified as the negative mass instability [3-5]. It induces uniform E layers to be azimuthally bunched, and beam energy is thereby transferred to wave energy. In most experiments with smooth conducting walls, the radiation spectra have shown many harmonic frequencies, e.g., harmonic numbers up to 40. Recently, the mode competition has been controlled by introducing multivane circuit similar to anode blocks in magnetrons [6]. In contrast to these relativistic devices, the cusptron uses low-energy, axis-rotating electron beams and a multivane circuit to control mode competitions [7-9].

Experimental Apparatus

The experimental setup of the NSWC cusptron is shown schematically in Fig. 1. The magnetic cusp field is produced by three independently controlled power supplies to the coils. The cusp transition width is narrowed substantially by a soft iron plate placed between the second and third coils. The transition length has been measured as 4.8 mm, which is determined by the FWHM of the radial magnetic field at the beam radius. The system vacuum is maintained by ion pumps at lower than 1×10^{-8} Torr.

† Work supported by the IR Fund at NSWC and by the Office of Innovative Science and Technology, the Strategic Defense Initiative Organization, managed by the Harry Diamond Laboratory.

NSWC CUSPTRON EXPERIMENT

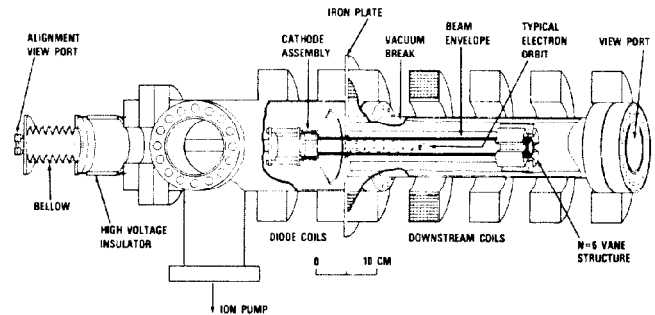


Fig. 1. Schematic of the NSWC cusptron experiment.

A hollow electron beam is produced from an annular thermionic cathode of 1.5 cm radius and 0.2 cm radial width with a Pierce type focusing electrode. The cathode assembly is mounted on a bellows coupled pipe for its alignment, and the cathode-anode gap can be adjusted without breaking system vacuum. An anode with an annular slit supported by three bridges is attached to an iron plate. A 0.2 cm wide annular slit allows the cylindrical beam to pass through the magnetic cusp transition region, where the $(v_z \times B_r)$ force converts effectively the beam axial velocity into the azimuthal velocity on the downstream side of the cusp transition. The downstream beam current is monitored by a pickup loop to a ground lead from the downstream chamber which is electrically insulated by a vacuum break. A six-vane circuit for the beam-wave interaction is placed at 4.0 cm downstream from the iron plate. This axial gap allows the beam envelope to be expanded in the cusp transition region without destruction. The circuit design is based on theoretical studies for the resonant interaction between an E layer of 25 keV and the sixth harmonic frequency [10-13].

Modes in Multivane Circuits

The six-vane RF circuit is utilized to encourage the sixth harmonic interaction (see Fig. 3 for its cross section). Due to the presence of the periodic interruptions in the azimuthal direction, the individual azimuthal mode number is no longer an eigen-number, and the cusptron RF eigenmode is an infinite sum of certain azimuthal modes in a circular cylinder. In order to emphasize this different grouping of the RF azimuthal modes, we devise a new convention of the (i,j) -mode designation. In this convention, the first number i is the primary azimuthal mode number that determines the phase difference of the neighboring resonators, and the two numbers i and j are the first two available RF azimuthal mode numbers. Also the sum of the two numbers represents the number of the vanes. In the six-vane circuit, there exist four different modes; the $(0,6)$, $(1,5)$, $(2,4)$, and $(3,3)$ -modes. The $(2,4)$ -mode can interact with either the second or the fourth harmonic frequencies. In magnetrons, the $(0,6)$ - and $(3,3)$ -modes are the 2π - and π -modes, respectively.

The peculiar property of the azimuthal mode mixture in this circuit may be understood with a simple argument given in Fig. 2, where the azimuthal electric

fields at openings of resonators are drawn. Here the azimuthal angle is linearly stretched for simplicity. The conducting wall forces the field to be vanished except for the openings. The fields at the openings are assumed to be constant, and the phase information is enforced via the primary azimuthal mode number. The eigenmodes thus obtained are shown with the solid line in the square wave forms. Obviously, these square waves can not be represented by a single sinusoidal wave, and the Fourier components of these square waves determine the amplitude of the partial azimuthal modes. The first two Fourier components are shown with broken and dotted lines. One notes that the different modes have different partial azimuthal modes, and they do not overlap. One also notes that the amplitude for the second partial mode is comparable to that for the first, e.g., 6 and 0 for the (0,6)-mode. For the present purpose, the (0,6)-mode has sufficient amplitude for azimuthal mode 6 to interact with the six bunches of the electron beam in producing the sixth harmonic.

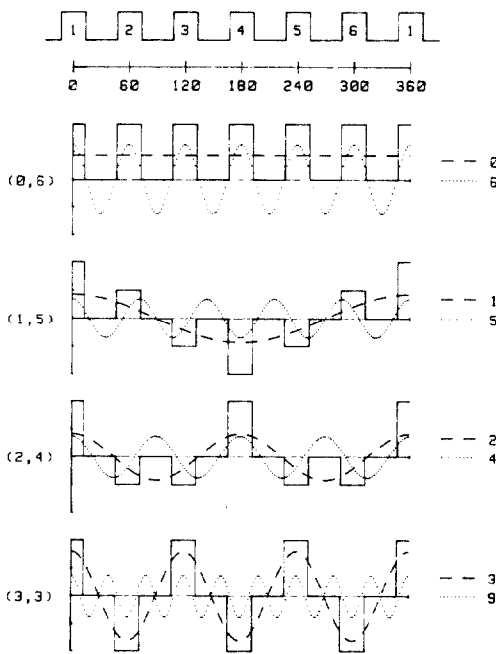


Fig. 2. Fields at the openings of the resonators.

The cross section and dimensions of the six-vane circuit are shown in Fig. 3 along with the vacuum dispersion relations and the interaction region in the magnetic field. The axial length of the circuit is 40 cm long with a slight tapered section at the front end. One notes from the dispersion curves in Fig. 3(c) that the (0,6)-mode is not the lowest frequency in the circuit, but it can be selected for the interaction by adjusting the magnetic field such that the sixth harmonic intercepts the dispersion curves as shown in Fig. 3(d), where the Doppler shift term of the beam modes is not taken into account for simplicity.

Experimental Results

The diode is operated at 25-30 kV, 4 μ s, 60 pps, and 0.6-1.0 μ serv. The current of the axis-rotating beam is typically 1.5-3.5 A depending on magnetic field configurations. The applied magnetic fields are 180-270 G in the diode region and 340-490 G in the circuit region. The block diagram for radiation diagnostics is shown in Fig. 4. Radiation is detected by a C-band standard gain horn antenna located beyond a circular pipe of 15 cm O.D. and 30 cm length which guides radiation from the downstream viewport to the receiving

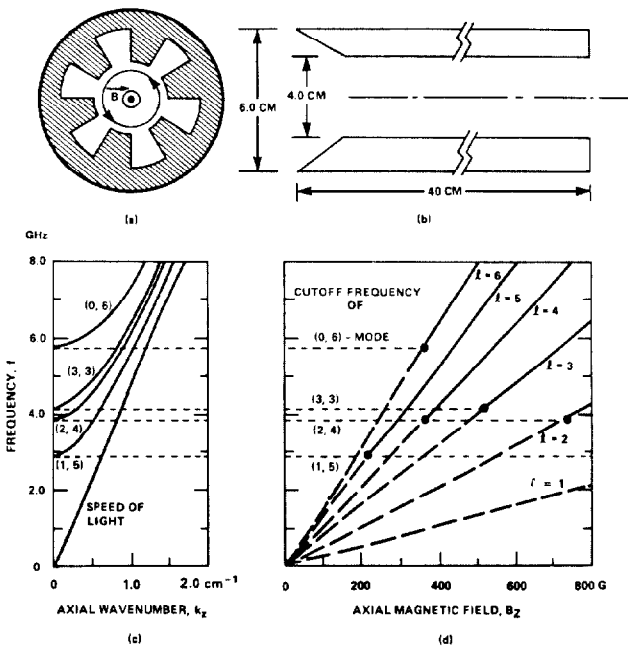


Fig. 3. (a) Cross section and (b) dimensions of the six-vane circuit, and (c) dispersion curves and (d) beam wave interaction region in magnetic fields.

horn antenna [8]. For the maximum gain configuration between the transmitting and receiving antennas, the horn antenna is positioned with a polar angle of 10-20° [8]. The radiation frequency is accurately determined by a storage spectrum analyzer (HP-8569B). The output power is measured by a power meter (HP-432B) and by a calibrated crystal detector from the attenuated signals. One notes that the total attenuation of microwave power to the crystal detector is more than 63 dB, since 60 dB is the sum of attenuators used, and 3 dB is from the polarization effect of the coupling between the circular polarization of the radiation fields and the linear polarization of the waveguide fields [8].

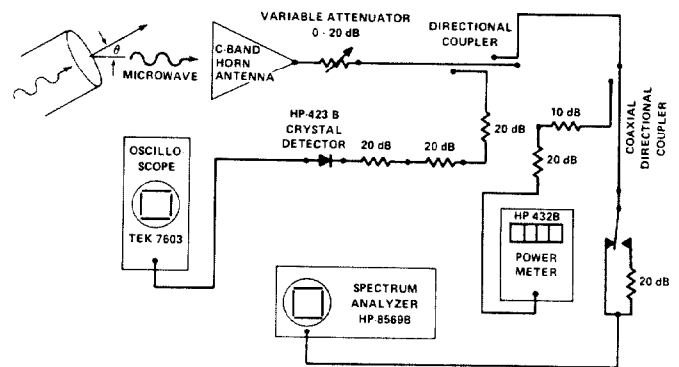


Fig. 4. Block diagram of radiation diagnostics.

There are two operating regimes in this setup. One generates radiation of more than 10.0 kW about 6.0 GHz, and the other yields 4.0 kW around 3.9 GHz from interactions with the sixth and fourth harmonics of the electron cyclotron frequency, respectively. They are separated slightly in the applied magnetic field strength in the circuit region.

The oscilloscope and the spectrum analyzer traces are shown in Fig. 5 and 6 for the (0,6)-mode excitation by the sixth harmonic interaction. In Fig. 5, the detector signal attenuated by more than 63 dB is 520 mV which corresponds to the microwave output power of approximately 10.4 kW (top trace). The current of the axis-rotating beam is 3.5 A (middle trace), and the beam energy is 30 keV (bottom trace). The electronic efficiency is about 10% in this case. The spectrum analyzer trace in Fig. 6 shows that the radiation frequency is 6.0 GHz with no other components in the 3.5-8.5 GHz band with the 60 dB dynamic range. For the sixth harmonic interaction at 6.0 GHz, the required magnetic field is only 380 Gauss.

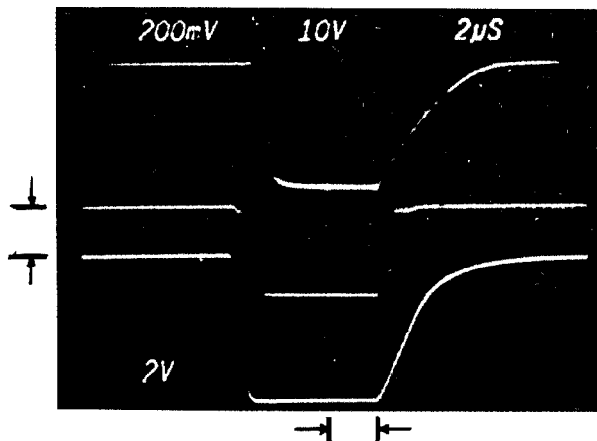


Fig. 5. Oscilloscope traces for the sixth harmonic frequency generation; (top) crystal detector (200 mV/div) of 63 dB attenuated signal of 10.4 kW, (middle) beam current of 3.5 A (2.0 A/div) and (bottom) beam energy of 30 keV (10 keV/div).

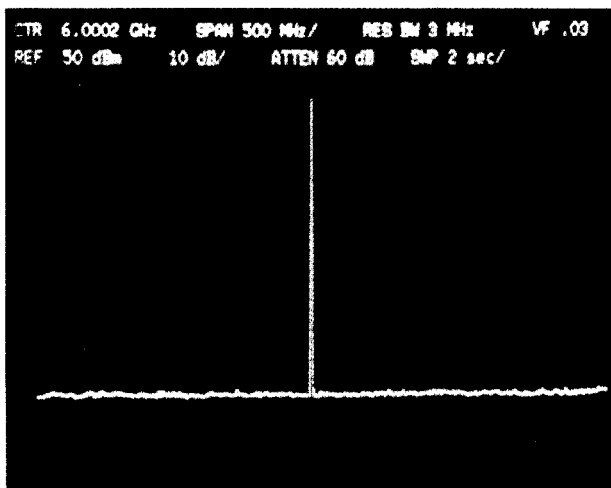


Fig. 6. Spectrum analyzer trace for the sixth harmonic frequency generation; the center frequency is 6.0 GHz with 500 MHz/div and 10 dB/div.

For the fourth harmonic interaction, the beam energy is 28 keV, and the downstream beam current is 1.5 A. Radiation power is approximately 4.0 kW at 3.9 GHz with an electronic efficiency of about 9.5%. The spectrum analyzer trace in Fig. 7 shows that it is the only frequency detected in the 3.5-8.5 GHz band. In both cases, radiation frequencies are a direct function of the magnetic field strength in the circuit region,

i.e., a tunable device as observed previously [8]. The range of frequency tuning is about 10% with respect to the cutoff frequency of each mode. We observed also that the magnetic field in the circuit region should be increased from that for the sixth harmonic case, while the magnetic field in the diode region should be decreased. It may be compared with the fact that the (2,4)-mode requires a slightly higher magnetic fields than that for the (0,6)-mode in Fig. 3(d).

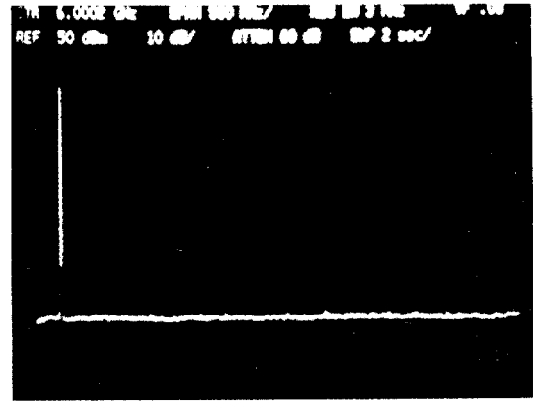


Fig. 7. Spectrum analyzer trace for the fourth harmonic frequency generation; the center frequency is 6.0 GHz with 500 MHz/div and 10 dB/div.

In conclusion, microwave radiation of 10.4 kW at 6.0 GHz has been generated by the sixth harmonic interaction of an axis-rotating beam of 30 keV and 3.5 A with the (0,6)-mode in a six-vane circuit. The electronic efficiency is approximately 10%. In addition, the fourth harmonic frequency has been generated with the same six-vane circuit. In this case, the (2,4)-mode has been excited by an axis-rotating beam of 28 keV and 1.5 A. The output power is approximately 4.0 kW at 3.9 GHz, and the electronic efficiency is 9.5%. The cusptron holds promise as an efficient, compact, and also tunable microwave tube suitable for many applications including high-power amplifiers for future accelerators [14].

References

- [1] N. C. Christofilos, et al., in *Proc. Conf. Plasma Phys. Controlled Nucl. Fusion Research* (IAEA, Vienna), Vol. 2, 211 (1966).
- [2] W. W. Destler, et al., *J. Appl. Phys.* **48**, 3291 (1977).
- [3] C. E. Nielson, et al., in *Proc. Int. Conf. on High-Energy Accelerators and Instrumentation*, (Geneva, Switzerland), CERN (1959).
- [4] P. Sprangle, *J. Appl. Phys.* **47**, 2935 (1976).
- [5] H. S. Uhm and R. C. Davidson, *J. Appl. Phys.* **49**, 593 (1978).
- [6] W. W. Destler, et al., *Appl. Phys. Lett.* **38**, 570 (1981).
- [7] W. Namkung, *Phys. Fluids* **27**, 329 (1984).
- [8] W. Namkung and J. Y. Choe, *IEEE Trans.* **NS-32**, 2885 (1985).
- [9] W. Namkung, et al., in *Conf. Digest 11th Int. Conf. Infrared Millimeter Waves*, 51 (1986).
- [10] H. S. Uhm, et al., *Phys. Fluids* **27**, 488 (1984).
- [11] Y. Y. Lau and L. R. Barnett, *Int. J. Infrared Millimeter Waves* **3**, 619 (1982).
- [12] K. R. Chu and D. Dialetis, *Int. J. Infrared Millimeter Waves* **5**, 37 (1984).
- [13] J. Y. Choe, et al., *Int. J. Electronics*, (to be published).
- [14] J. Y. Choe and W. Namkung, *IEEE Trans.* **NS-32**, 2882 (1985).